

N89-19262

TURBOMACHINERY AEROELASTICITY AT  
NASA LEWIS RESEARCH CENTER

Krishna Rao V. Kaza  
Structural Dynamics Branch  
Structures Division  
NASA Lewis Research Center  
Cleveland, Ohio

The turbomachinery aeroelastic effort at NASA Lewis Research Center is focused on unstalled and stalled flutter, forced response, and whirl flutter of both single-rotation and counter-rotation propfans (figs. 1 & 2). It also includes forced response of the space shuttle main engine (SSME) turbopump blades (fig. 1). Because of certain unique features of propfans and the SSME turbopump blades, it is not possible to directly use the existing aeroelastic technology of conventional propellers, turbofans or helicopters. Therefore, reliable aeroelastic stability and response analysis methods for these propulsion systems must be developed. The development of these methods for propfans requires specific basic technology disciplines, such as 2D and 3D steady and unsteady (unstalled and stalled) aerodynamic theories in subsonic, transonic and supersonic flow regimes; modeling of composite blades; geometric nonlinear effects; and passive or active control of flutter and response. These methods for propfans are incorporated in a computer program ASTROP (fig. 3). The program has flexibility such that new and future models in basic disciplines can be easily implemented. The forced response analysis method for turbine blades will be discussed later.

### UNSTEADY AERODYNAMICS AND AEROELASTICITY

SR LARGE SCALE  
AERODYNAMICS AND FLUTTER  
SR 7 L



SR-3 RESEARCH MODEL  
FLUTTER, FORCED  
RESPONSE, AND MISTUNING



CR PROPFAN WIND TUNNEL MODEL  
AERODYNAMICS AND FLUTTER



SSME TURBOPUMP BLADE  
FORCED RESPONSE

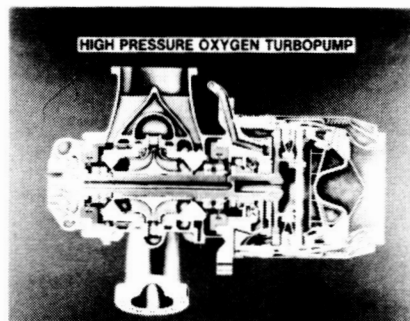
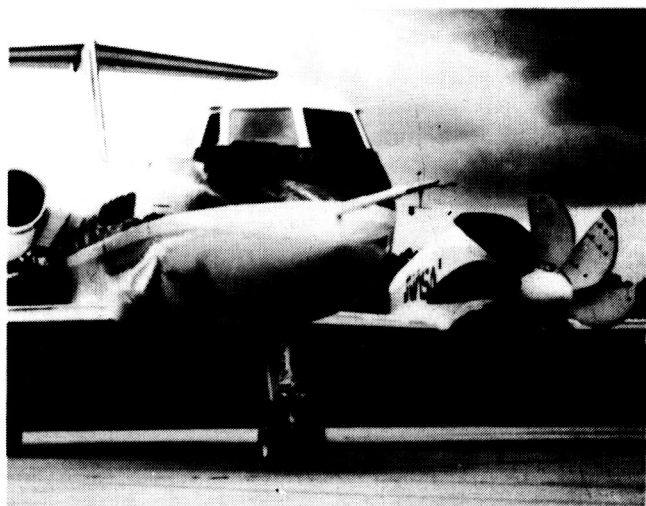


Figure 1

ORIGINAL PAGE IS  
OF POOR QUALITY

## UNSTEADY AERODYNAMIC AND AEROELASTICITY FLIGHT TEST PROGRAM

SR PROPFAN



CR PROPFAN



Figure 2

ASTROP

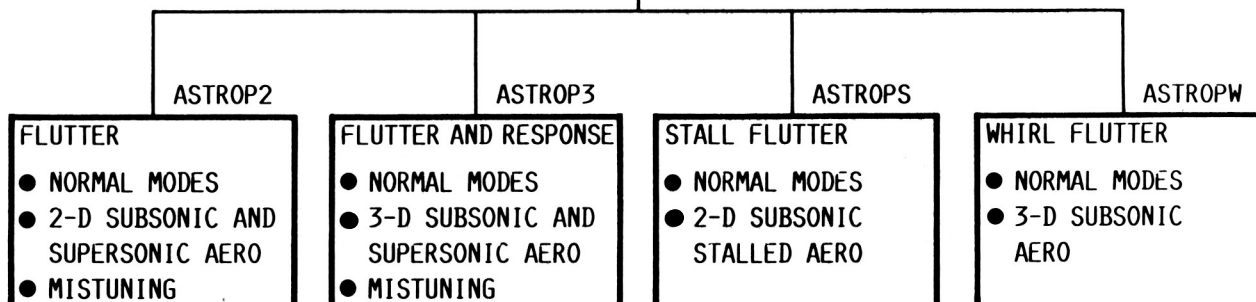
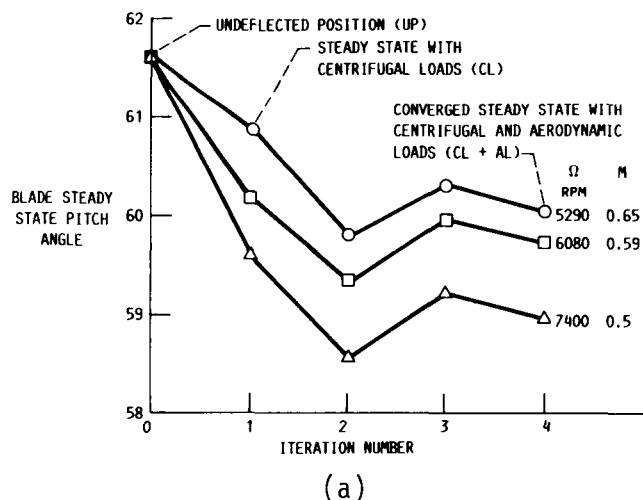


Figure 3

## Application of the ASTROP Code to Investigate Flutter of a Composite SR Propfan Model

One version of the code called ASTROP3 (ref. 1) uses three-dimensional subsonic steady and unsteady cascade aerodynamics (ref. 2) and NASTRAN (ref. 3) finite element model to represent the blade structure. The equivalent anisotropic material properties for each finite element are generated by using a preprocessor code COBSTRAN (ref. 4). The effect of centrifugal loads and steady-state airloads on the steady-state geometry of a composite wind tunnel model (SR3C-X2) blade is shown in figure 4(a). The aerodynamic cascade effects (or the effect of number of blades) on the eigenvalues are shown in figure 4(b). Both centrifugal loads and aerodynamic loads untwist the blades and this untwist increases with rotational speed. It is evident from figure 4(b) that the number of blades or the cascade effect is very significant on the real part of the eigenvalue and hence on stability.

**EFFECT OF CENTRIFUGAL AND AERODYNAMIC LOADS ON  
BLADE PITCH ANGLE**



(a)

**EFFECT OF NUMBER OF BLADES ON EIGENVALUES**

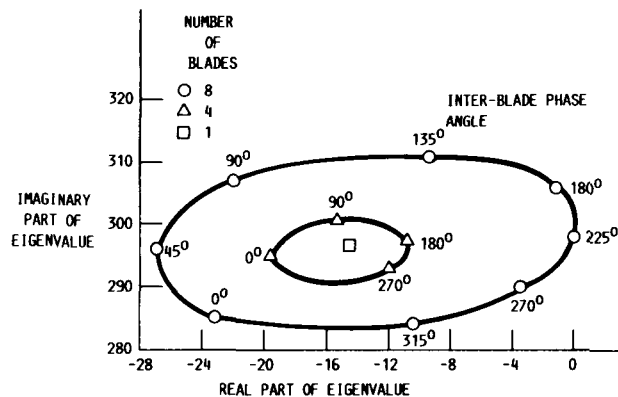
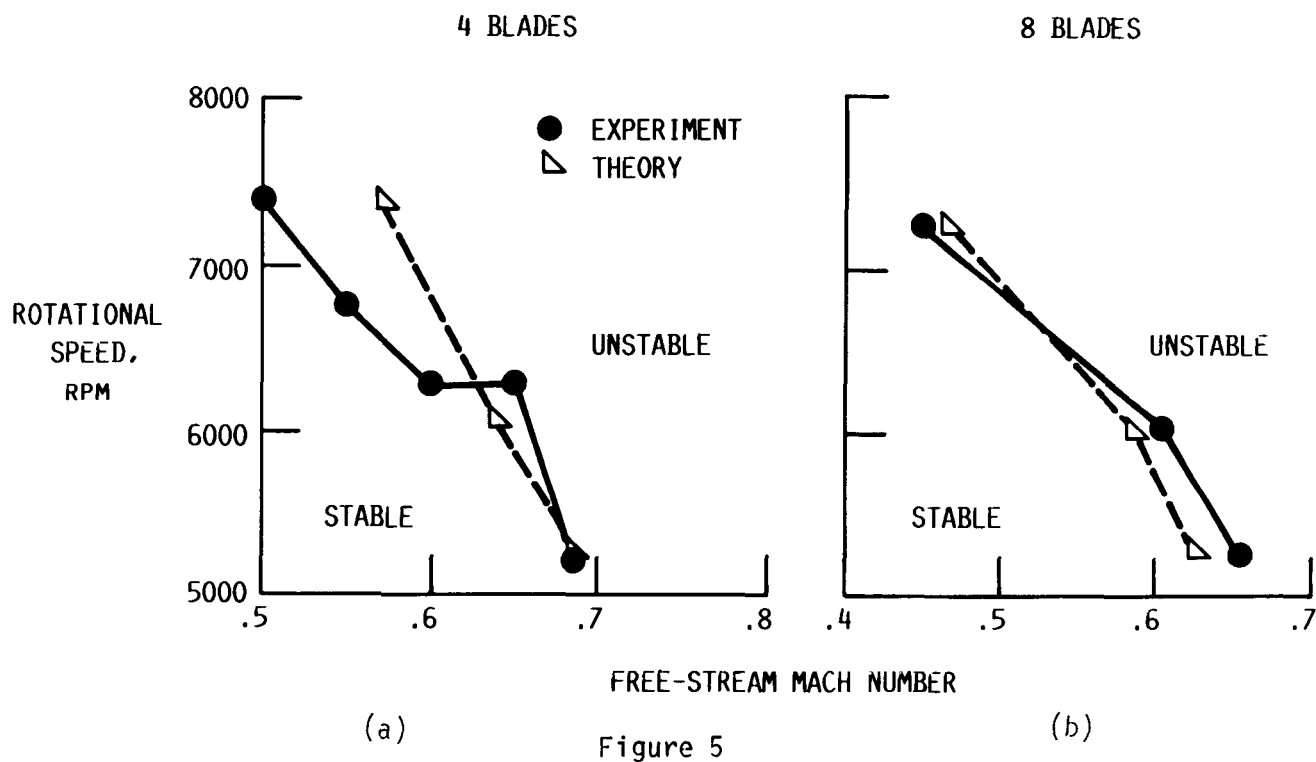


Figure 4 (b)

Comparison of Measured and Calculated Flutter  
Boundaries for the SR3C-X2 Propfan Model

Theoretical flutter results obtained from the ASTROP3 code have been correlated in figures 5(a) and (b) with flutter data of a wind tunnel propfan model (ref. 5), SR3C-X2, with composite blades. Theoretical results include the effects of centrifugal loads and steady-state airloads. The theory does reasonably well in predicting flutter speeds and slopes of the boundaries. However, the difference between the calculated and measured flutter Mach numbers for the four-blade case is greater than for the eight-blade case. This implies that the theory may be overcorrecting for aerodynamic cascade effects for four blades. Calculated interblade phase angles at flutter (not shown) also compared well with measured values. However, calculated flutter frequencies were about 8% higher than measured.



## Evaluation of Two-Dimensional Unsteady Aero for Propfan Flutter Prediction

Actually the ASTROP code was started with two-dimensional unsteady aerodynamic theory (ref. 6) by correcting for blade sweep (ref. 1). The version of the code which uses blade normal modes and two-dimensional unsteady aero theory in a stripwise manner is ASTROP2 (figure 3). The ASTROP3 version uses three dimensional unsteady aero theory. To assess the validity of two-dimensional aerodynamic theory and the associated sweep correction, the real part of the eigenvalue of the critical mode calculated by using both ASTROP2 and ASTROP3 are compared in figure 6. Also included in this figure is the measured flutter mach number. Evidently, the two-dimensional theory is less accurate than three-dimensional theory in predicting flutter Mach number for this case. Correlative studies (not shown) of measured and calculated flutter boundaries were also conducted by varying Mach number, blade sweep, rotational speed, and blade setting angle. The correlation varied from poor to good. In some cases the expected conservative nature of the two-dimensional theory did not prevail, possibly because of the arbitrary nature of the reference line which is employed in the strip-method, and the associated sweep correction.

### COMPARISON OF 2-D AND 3-D UNSTEADY AERO FOR PROPFAN FLUTTER PREDICTION

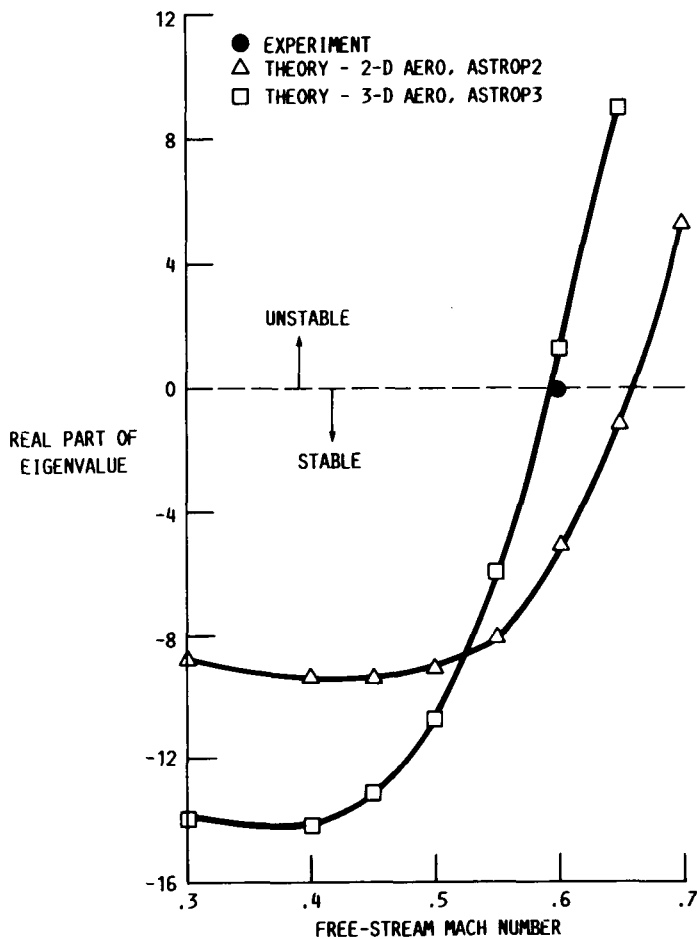
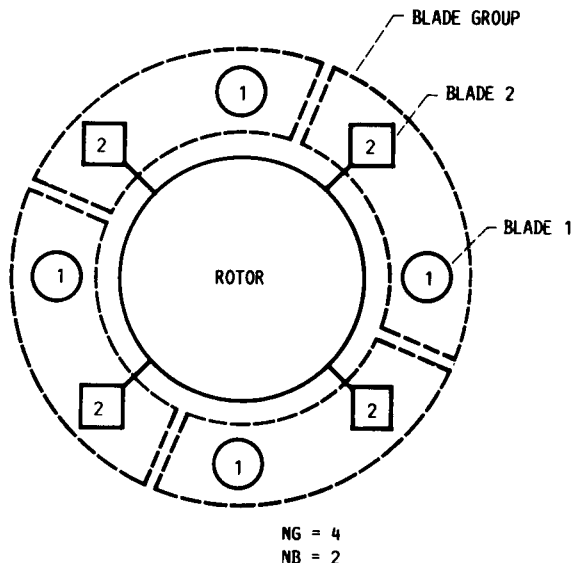


Figure 6

## Propfan Blade Mistuning Models

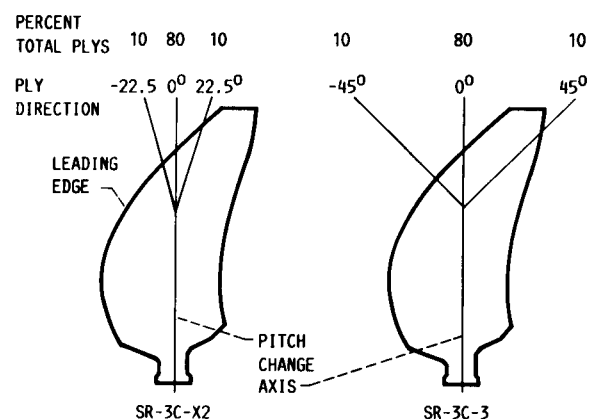
Understanding the effects of blade mistuning on vibration, flutter and forced response of turbomachinery rotors is a current research topic because mistuning affects flutter and response behavior. An analytical and experimental investigation of mistuning in propfan flutter was conducted in ref. 7. A schematic for an eight-bladed mistuned rotor in formulating the analytical model and blade ply directions used in constructing the wind tunnel model are shown in figures 7 (a) and (b), respectively. The analytical model, which is more general than the wind tunnel model, is based on normal modes of a rotating composite blade and subsonic unsteady lifting surface aerodynamic theory. The natural frequencies and mode shapes of the SR3C-X2 and -3 model blades differ because of the ply angle variations between the blades. The first mode frequencies of both the blades are very close and were insensitive to ply angles. However, the average second mode frequency of the SR3C-3 blade is about 12 percent higher than that of the -X2 blade. More details can be found in ref. 7.

**BLADE GROUP SCHEMATIC FOR AN EIGHT-BLADED ROTOR**



(a)

**BLADE PLY DIRECTIONS**



(b)

**Figure 7**

### Comparison of Eigenvalues of Tuned and Mistuned Propfan Models

To illustrate the effect of mistuning (which is partly aerodynamic and structural) the calculated real and imaginary parts of eigenvalues of the SR3C-X2 (8-bladed tuned rotor), SR3C-3 (8-bladed tuned rotor), and mixed (mistuned) rotor were compared in figure 8. The mistuning is due to the differences in blade steady-state geometry, frequencies, and mode shapes. The eigenvalues are for all interblade phase angles of the mode with lowest damping. The calculations were performed by treating the SR3C-X2 and -3 rotors as tuned and the mixed rotor as an idealized alternately mistuned rotor--four identical blade pairs with two different blades in each pair. Comparison of root loci indicates that the area of the approximate ellipse for the SR3C-X2 is greater than that of SR3C-3, indicating a stronger aerodynamic coupling between the blades of the SR3C-X2 rotor. The difference in stability of the tuned rotors is due to the difference in blade stiffness and mode shapes because of the different ply angles of the blades. The results also show that mixing the blades significantly affected the eigenvalues and resulted in a rotor with a greater damping than the lowest damped mode of either tuned rotor.

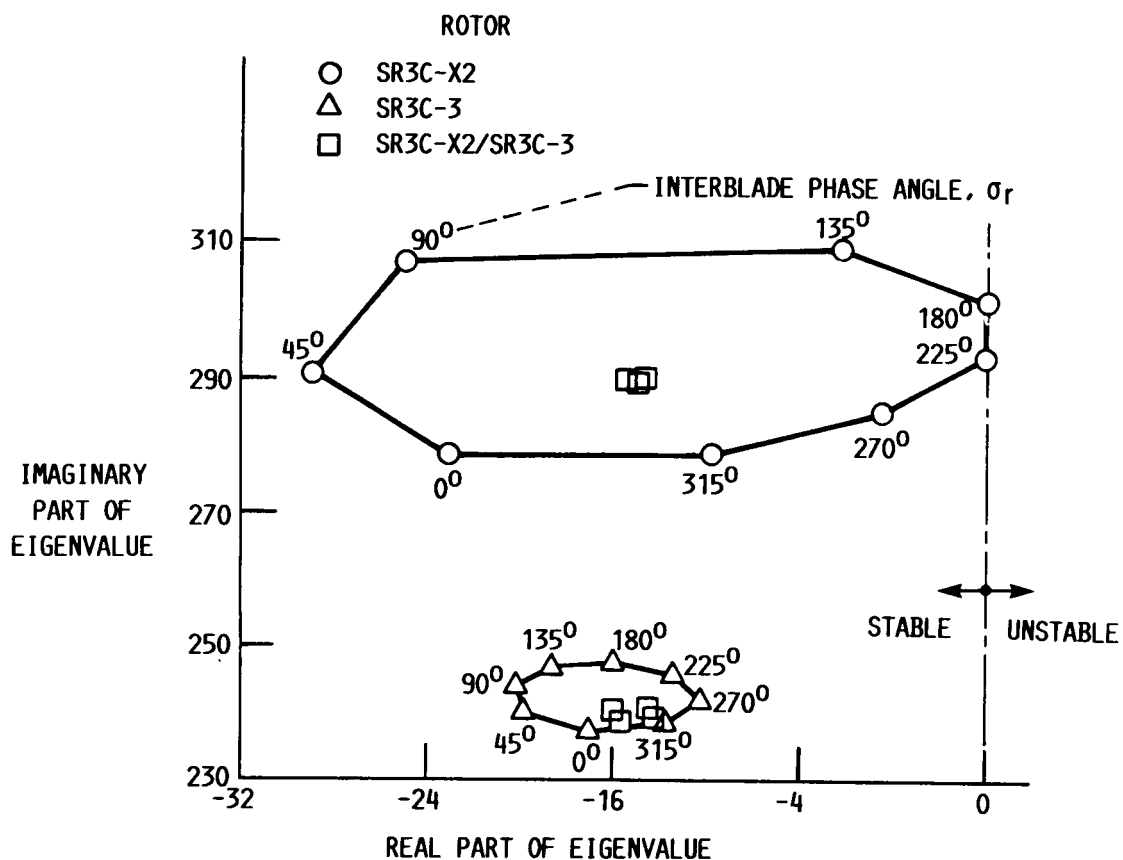


Figure 8

### Comparison of Measured and Calculated Flutter Boundaries for Tuned and Mistuned Propfan Models

Measured and calculated results for the tuned rotor SR3C-X2 and mistuned rotor SR3C-X2/SR3C-3 are compared in figure 9. The calculations for each rotor were made with the calculated modes and frequencies, except that the measured second mode frequency was substituted for the calculated one. The calculated flutter Mach numbers for the SR3C-X2 are less than the measured ones for all rotational speeds. The agreement would be better if the effects of steady airloads and structural damping were included in calculations (see ref. 1 for detailed discussion). The agreement of the mixed rotor is better, but would become unconservative if steady airloads and structural damping were included in the theory. However, the overall agreement between theory and experiment is more than satisfactory. For additional details and results see ref. 7.

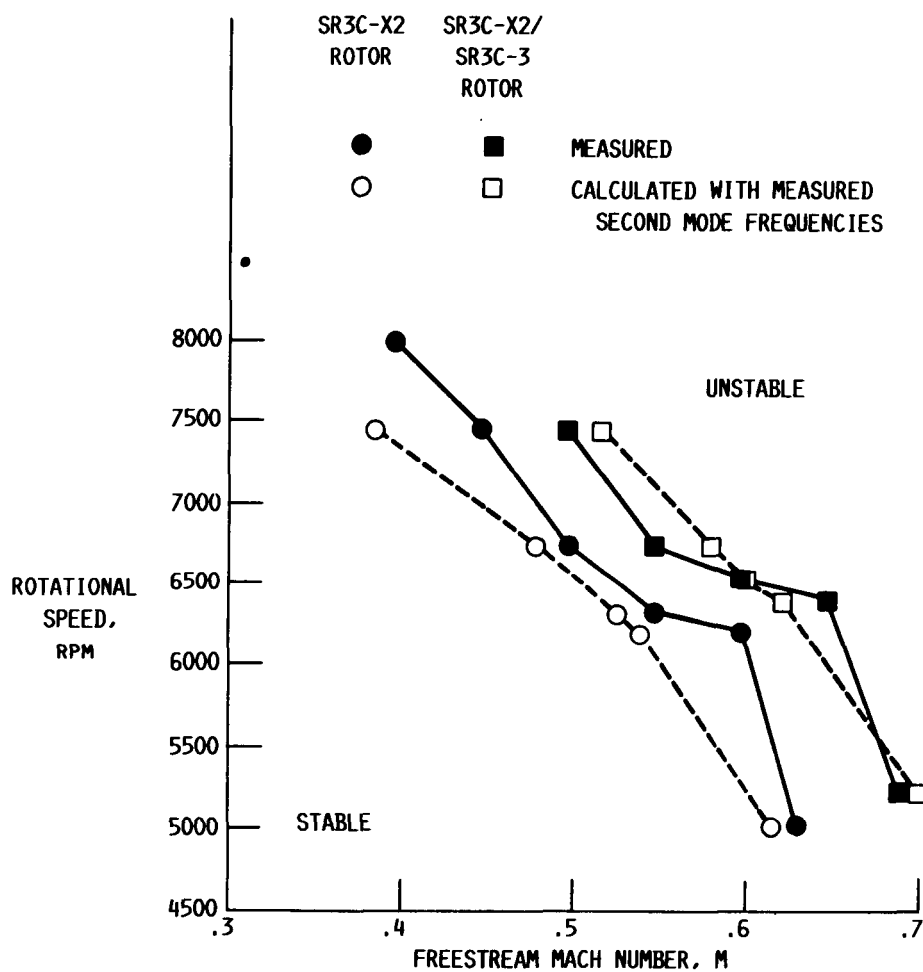
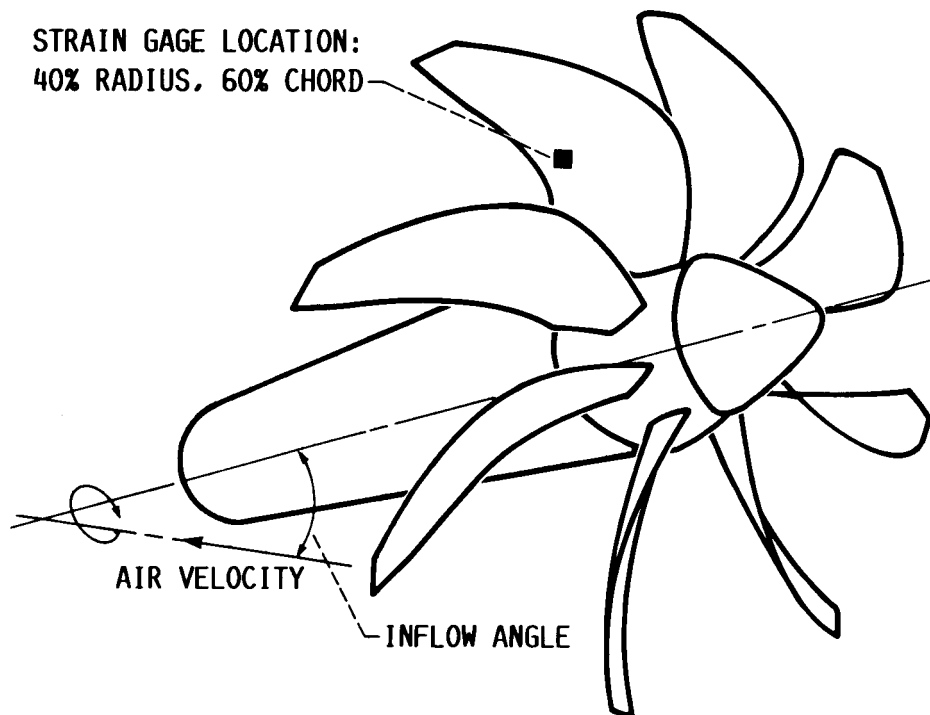


Figure 9

### Comparison of Measured and Calculated Vibratory Stress Amplitudes of a Propfan Model

A new feature of the ASTROP3 code under development is the capability to perform a modal forced response vibration analysis of aerodynamically excited propfans. Figure 10 depicts a single-rotation, advanced propfan wind tunnel model (SR5, 10 metallic blades), ref. 8, operating in a generally uniform, steady inflow field, inclined at a small angle with respect to the axis of rotation. Although the absolute inflow field is constant, rotation of the propfan results in velocities with oscillatory components relative to the blades. Under such conditions, ASTROP3 is able to determine the oscillatory loading distributions over the propfan blades at various excitation frequencies and calculate the vibratory displacements and stresses of the propfan. The table shows measured and preliminary calculated one per rev vibratory stress amplitudes for the SR5 blade. Also included in the table are the calculated results from ref. 9 by using a 2-D unsteady aerodynamic theory. Comparison shows that 2-D results are better than 3-D results. The reason for this difference is being investigated.



MEASURED STRESS, PSI	ASTROP3 PREDICTED	REFERENCE 9 PREDICTED
3365	2322	3065

Figure 10

## Stall Flutter Analysis Methods

The third feature of the ASTROP code is a stall flutter analysis which is in ASTROPS. Under take-off conditions, the propfan blades operate at high angles of attack and have the potential to stall flutter, triggered by separated flow during part of every cycle of oscillation. Stall flutter speeds are very low and the forces due to vibration at the stall condition (dynamic stall) are an order of magnitude high compared to forces in separated flow with no vibration. Prediction of forces during dynamic stall has been a continuing research effort. Some prediction methods are reviewed in ref. 10, and their classification is shown in figure 11. The Navier-Stokes solvers (N.S.S.), vortex methods, and the zonal methods attempt to solve the fluid mechanics equations in their fundamental form by numerical techniques with varying degrees of simplifications and assumptions. These models require a significant amount of computer time and therefore are not suitable for routine aeroelastic analysis. In semi-empirical models an analytical approximation is attempted to approximately reproduce measurements for example, by way of analytical curve fit to wind tunnel data. The semi-empirical models take less computer time to solve and can be used in a routine aeroelastic analysis.

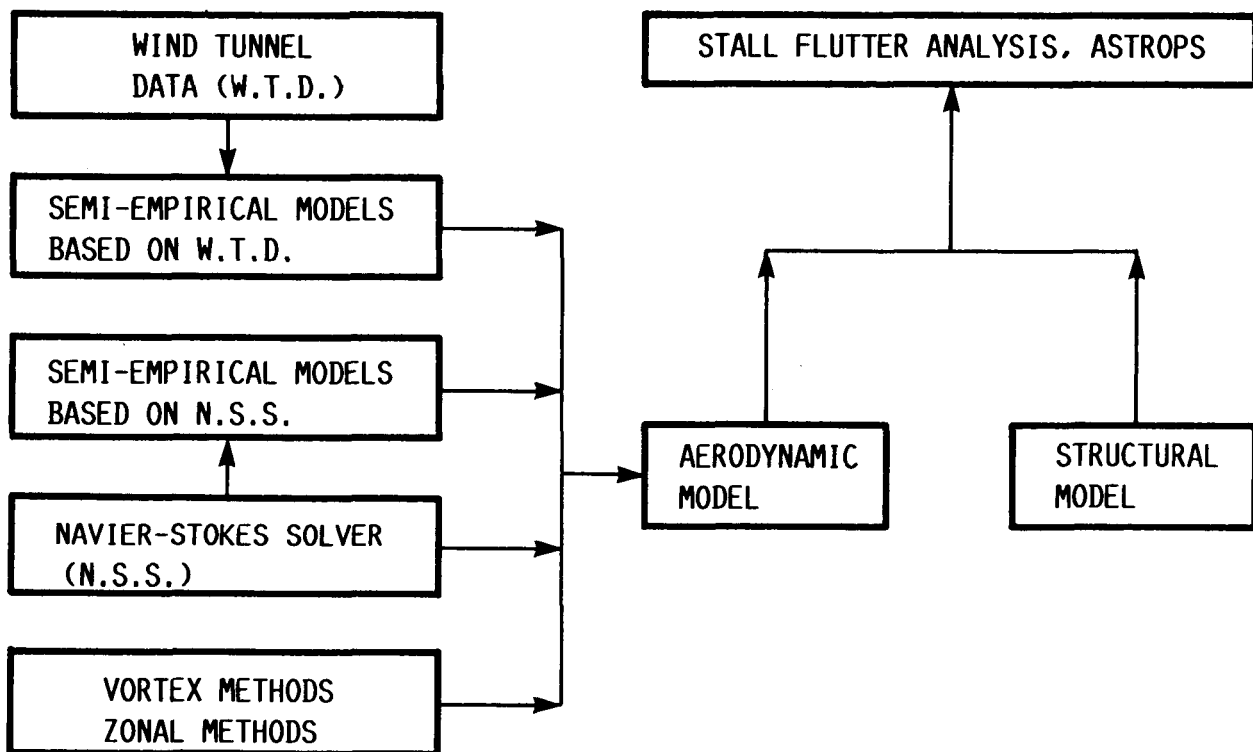


Figure 11

## Comparison of Measured and Calculated Stall Flutter Results of an Unswept Propfan Model

Recently two semi-empirical dynamic stall models, designated as model A and model B, were applied to an unswept propfan model (SR-2, 8 metallic blades). The calculated logarithmic decrement of third mode response as a function of blade pitch angle is shown in figure 12. Also included in the figure is the blade pitch angle at which the blade is unstable in a wind tunnel experiment. Model A (ref. 11) incorporates the unsteady effects in stall using only one stall parameter that relates the dynamic stall angle and the non-dimensional rate of angle-of-attack. The stall parameter is given as a function of Mach number and airfoil thickness to chord ratio. Model B (ref. 12) is a synthesized data method to dynamic stall modeling. An analytical curve is fitted for the wind tunnel data obtained from oscillating airfoil tests. The empirical parameters in the model are obtained from this fit. However, experimental dynamic data is not available for propfan airfoil sections (16 series). Therefore, in implementing model B for propfan application, the dynamic data corresponding to NLR-1 airfoil was used, even though the airfoil geometries are different. However, for the case studied here, the Mach number range for which the data available for the NLR-1 airfoil corresponds to the helical Mach number (at zero freestream Mach number) due to rotation of the propfan model. In spite of the differences in dynamic data, the empirical models chosen predicted a qualitative stall flutter behavior for the case studied. Both the models predicted that the stall flutter response occurred in third mode as was found in the experiment at a rotor speed of 8500 rpm. However, the calculated blade pitch angles at which the stall flutter occurred is lower than that of the experiment ( $30^\circ$ ), model B predicted a closer value ( $28.25^\circ$ ) compared to that predicted by model A ( $25^\circ$ ). The calculated frequency at stall flutter condition is about 10% higher than the experimental data.

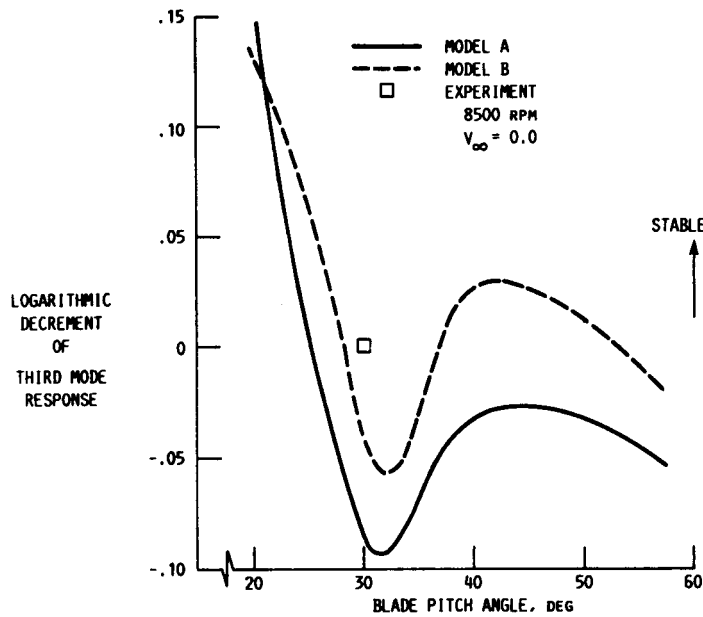


Figure 12

## Stall Flutter Analysis with Navier-Stokes Code

A solution procedure is described for determining the two-dimensional, one- or two-degree-of-freedom flutter characteristics of arbitrary airfoils at large angles-of-attack (see ref. 12). The same procedure is used to predict stall flutter including separated flow. This procedure requires a simultaneous integration in time of the solid and fluid equations of motion. The fluid equations are the unsteady compressible Navier-Stokes equations, solved in a body-fitted moving coordinate system using an approximate factorization scheme. The solid equations are integrated in time using an Euler implicit scheme. Several special cases, figures 13-15, are presented to demonstrate the capability of this scheme to predict transonic flutter and stall flutter with large separated flow.

The first case is shown to illustrate the capability of the present solver to predict the highly separated flows. The aerodynamic coefficients of an NACA 0012 airfoil oscillating in pitch at large angle-of-attack is shown and compared with experiment in figure 13. The mean angle and amplitude of oscillation was 15 degrees and 10 degrees respectively. The reduced frequency based on semi-chord was 0.151. The freestream Mach number and Reynolds number were 0.283 and 3.45 million respectively. It is seen from figure 13 that the Navier-Stokes solver produces lift, drag, and moment coefficients which are in a reasonable agreement with the measured ones. The fact that the flow solver is able to capture much of the dynamic stall flow features increases the confidence in the capability of this code for stall flutter predictions.

STALL FLUTTER ANALYSIS WITH NAVIER-STOKES  
 CODE:  $\alpha = 15 - 10 \cos(\Omega t)$

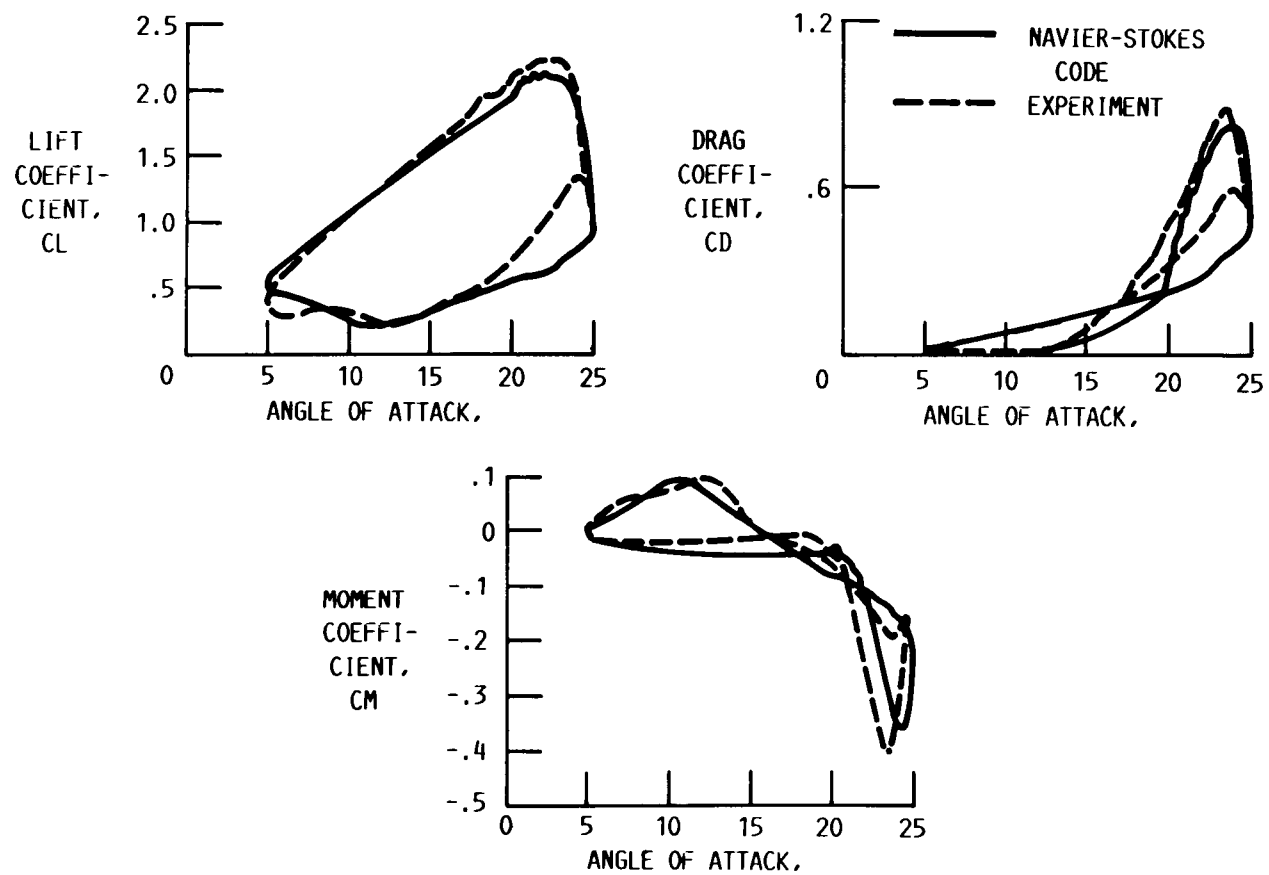


Figure 13

Comparison of Flutter Speeds from Euler, UTRANS2,  
and LTRAN2 Codes

A second special case considered for validation of the Navier-Stokes solver is its Euler version to calculate transonic flutter speed. Predicted transonic flutter speeds at various mass-to-air ratios for NACA 64006 airfoil oscillating in pitch and plunge at Mach number 0.85 are shown in figure 14. Several other validation cases are reported in ref. 13. The results from UTRANS2 (ref. 14) and LTRAN2 (ref. 15) are also included. Very good agreement between present Euler and UTRANS2 code results is found. A qualitative agreement between present and LTRAN2 results is found, too.

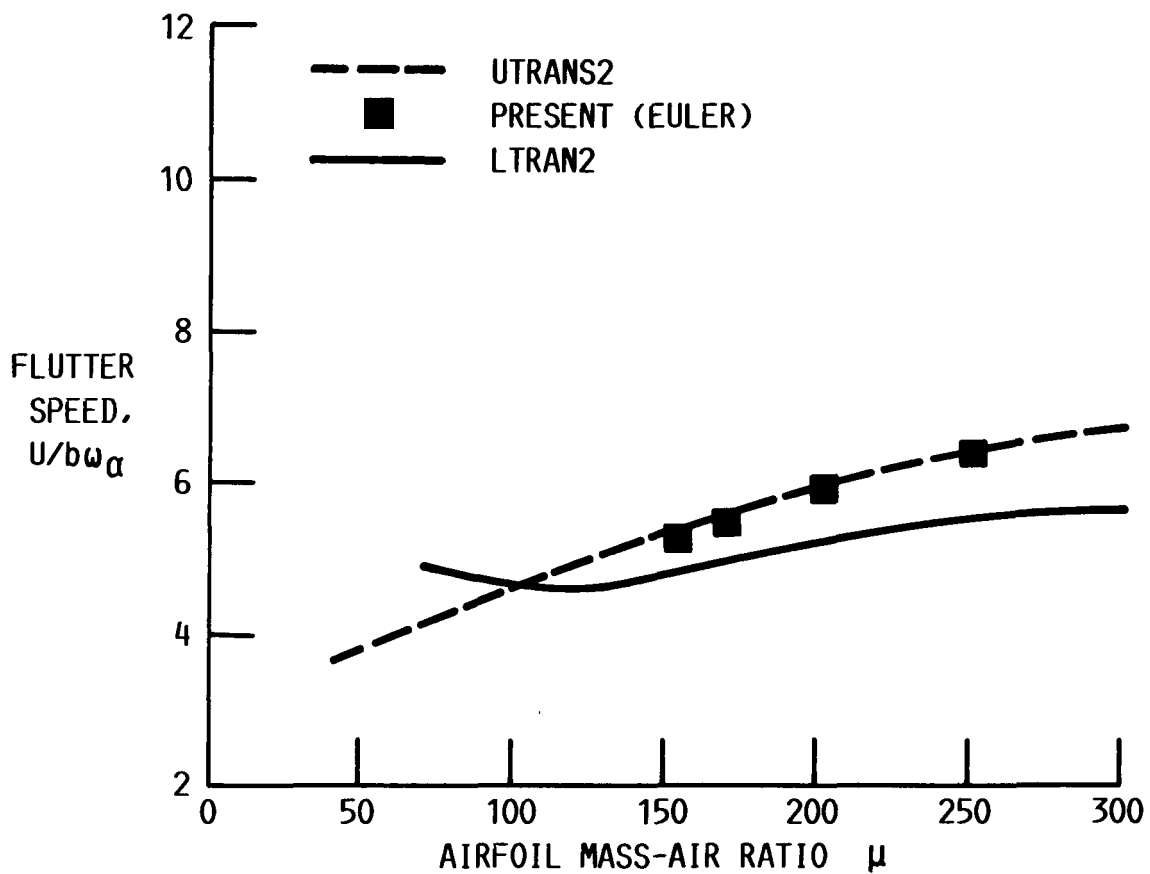


Figure 14

### Plunging and Pitching Stall Response

The third case considered with the Navier-Stokes code is the prediction of flutter at large mean angle-of-attack, including flow separations. The time response of plunging and pitching displacements and lift and moment coefficients of an NACA 0012 airfoil is shown in figure 15. The airfoil was initially subjected to a sinusoidal pitching oscillation from 5 to 25 degrees. During the downstroke, around 23.8 degrees, the airfoil was released and was allowed to follow a pitching and plunging motion. The dimensionless speed is varied from 4 to 8. The response of the airfoil is stable when the speed is 4 and is unstable when the speed increases to 8. It was found that the growing response is induced by the separated flow over the airfoil at large angle-of-attack.

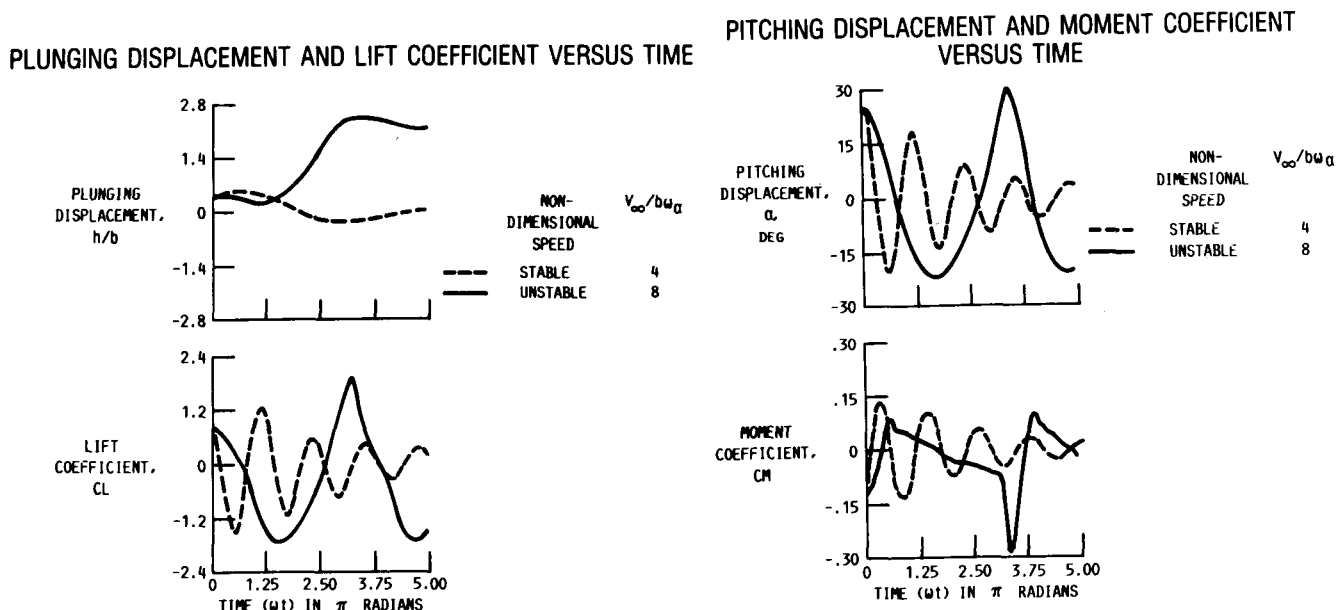


Figure 15

ORIGINAL PAGE IS  
OF POOR QUALITY

## Full Potential Unsteady (Cascade) Aero Model

A compressible, unsteady, full potential, finite difference code is being developed for modeling 2D/3D flow through single rotation propfans and other turbomachinery rotors. The procedure introduces a deforming grid with a uniform shear mesh. The numerical scheme is based on finite volume and implicit time marching technique. The 2-D code is vectorized and verified by applying it to several special cases. Two such cases are shown in figure 16. For comparison, the results from refs. 16 and 17 are also included. Even though a very coarse grid is used in the present calculations, the agreement between the present results and those of refs. 16 and 17 is very good. Validation of 3-D code is in progress.

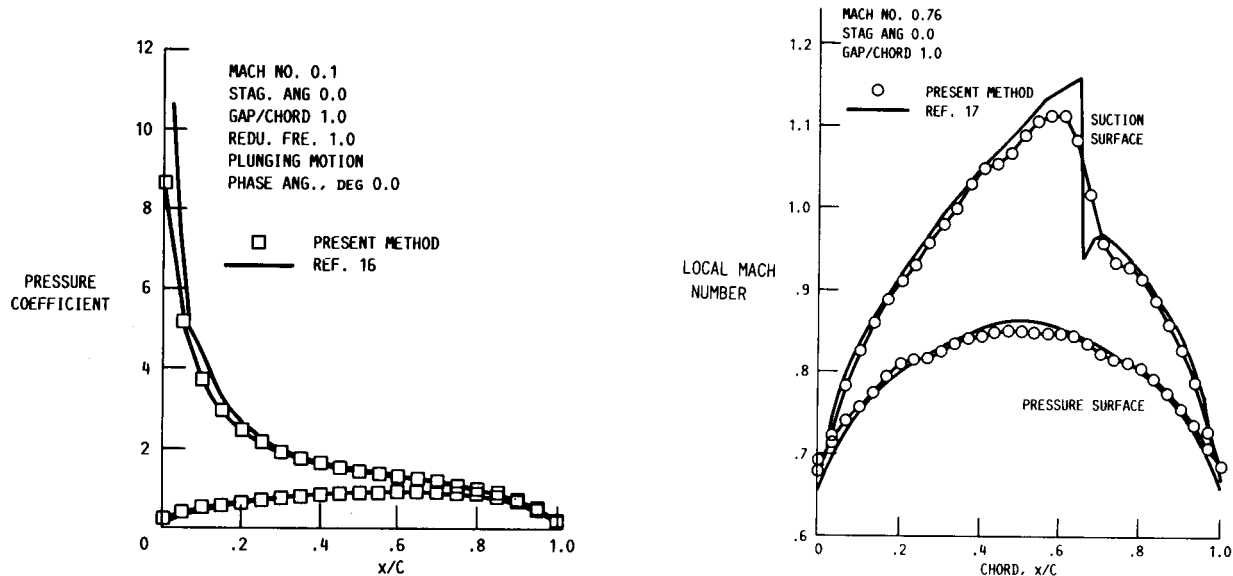


Figure 16

### CR Propfan 3-D Steady and Unsteady Aero Model

An incompressible, steady and unsteady aerodynamic model is being developed in ref. 18 for modeling flow through counter rotation propfans. The model is based on time domain solution in conjunction with panel method. This model is applicable for calculating performance and stability of both single and counter rotation propfans including interaction from wing. The code is being verified by applying to several special cases. One such case is shown in figure 17 in which present results are compared with the corresponding ones in ref. 19. See ref. 18 for additional validations and for details. This code will be extended to compressible flow, and, then, will be merged with ASTROP code structural modules to predict flutter of counter rotating propfans.

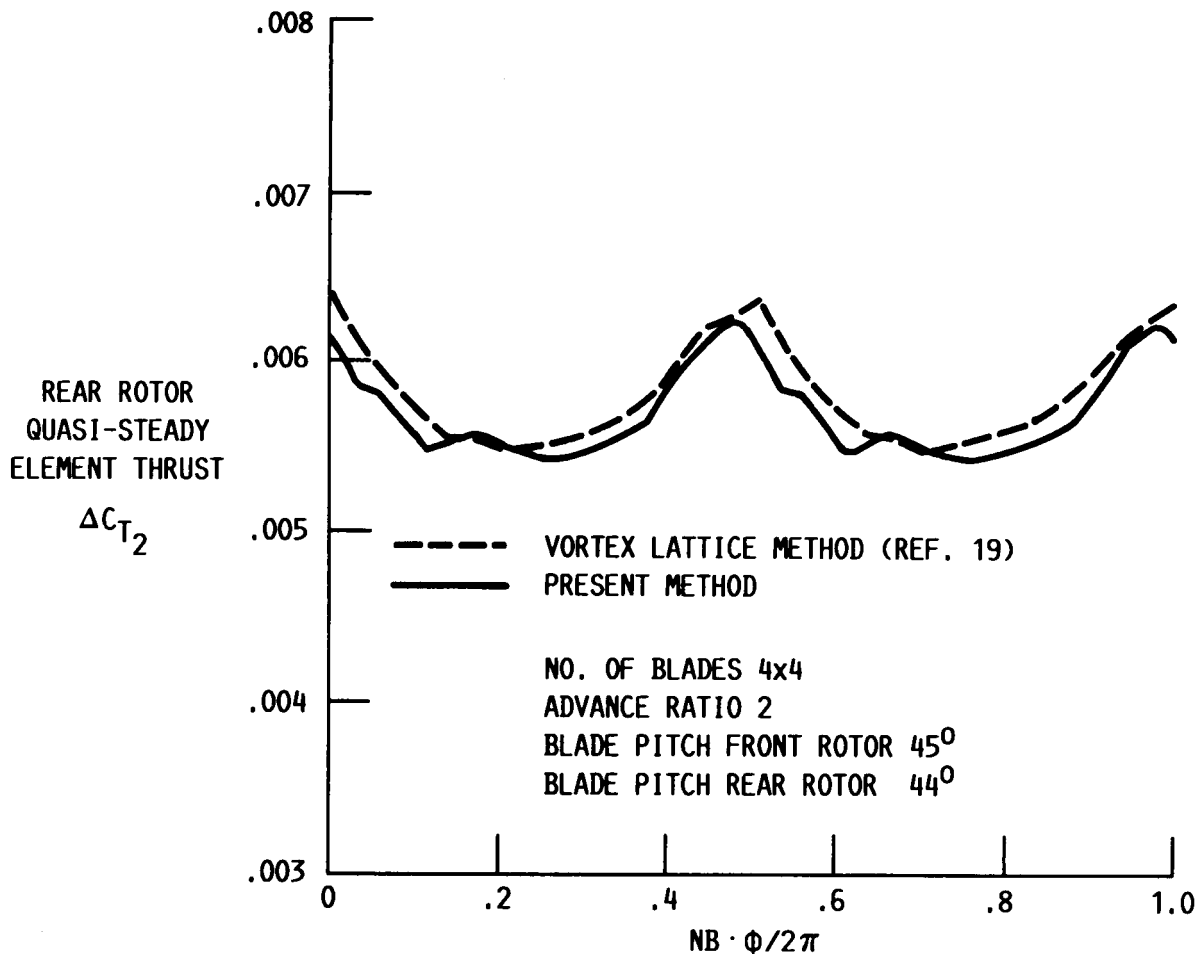


Figure 17

### Propfan Wind Tunnel Flutter Models

Figure 18 shows propfan blade wind tunnel models that have had flutter. These blades are not aeroelastically scaled models and were made for aerodynamic performance tests. However, the SR3C-X2 and -3 models were specifically designed for flutter and forced response experiments, respectively. One single rotation model had stall flutter, SR-2. The other two had unstalled flutter SR3C-X2 and SR-5. The flutter data from these models has been used to verify the analysis methods discussed earlier. The three counter-rotation models shown have had unstalled flutter. The correlation of this data with analysis is in progress.

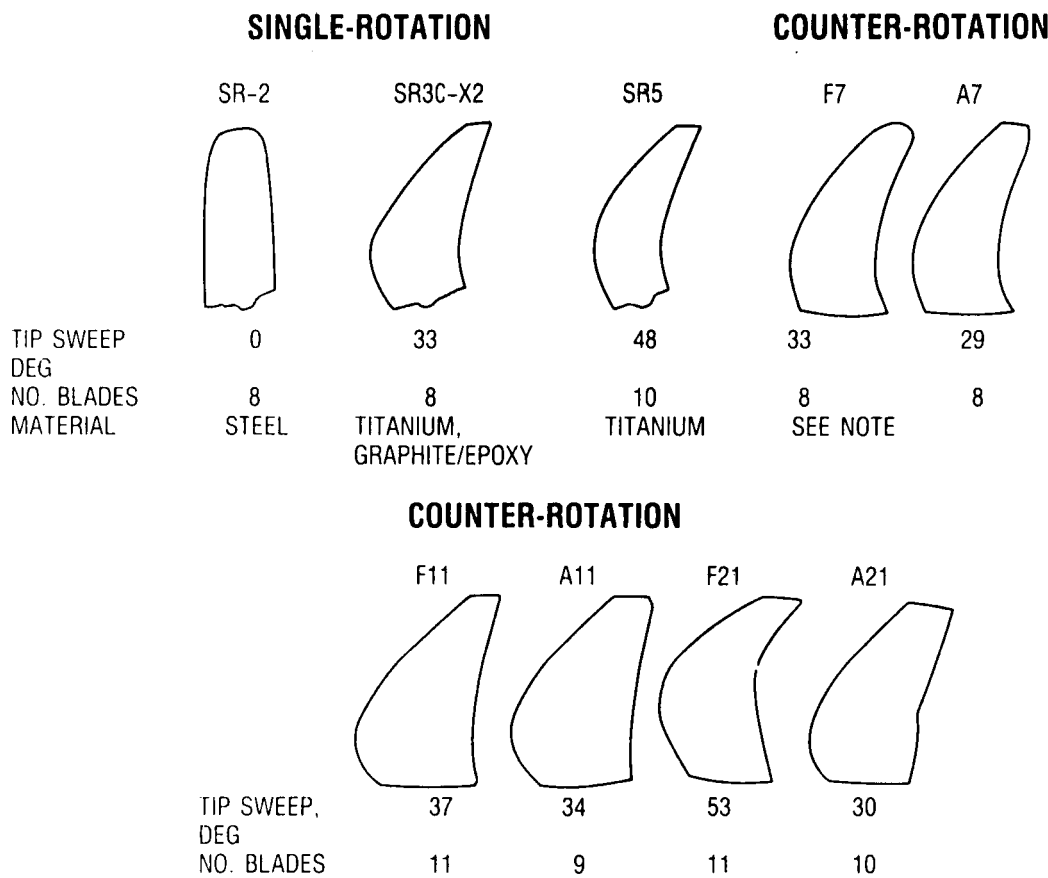


Figure 18

## Forced Response of SSME Turbopump Blades

The state-of-the-art in forced response analysis of turbomachinery blading is to simply calculate the blade natural frequencies and try to avoid known forcing frequencies (Campbell Diagram). Forced response calculations are not attempted. This can lead to unexpected blade cracking. The objective of this research is to develop a forced response prediction method for turbopump blades. The flow chart for this method is shown in figure 19. The development will proceed in three parallel, integrated tasks. The first task continues existing in-house research to develop a model (M-STAGE) of the 3D, time-averaged, flow field within a passage of a blade row embedded in a multi-stage machine. This model identifies the distorted (i.e. non-axisymmetric) flow field generated by neighboring blade rows. This information serves as input to Task 2. The second task will develop a model (LINPOT) to predict the unsteady aerodynamic loads generated by the flow distortion. This model will consist of an unsteady, linearized, potential flow solver, and a linearized, convected gust solver. The model will be applicable to thick, highly cambered turbine blades. The third task continues existing in-house research to develop a model (FREPS) for integrated forced response predictions. This model will integrate the M-STAGE model of task 1 with the LINPOT model of task 2 and a structural dynamic model. Two structural dynamic models will be used. Initially, a simplified two degree-of-freedom blade model will be incorporated. This will be followed by a complete modal blade model. The result of this research will be a system to calculate the forced response of a turbopump blade embedded in a multi-stage turbine. The benefit will be a marked reduction in occurrences of unexpected blade cracking. This system will also be applicable to blading in aeronautical propulsion systems.

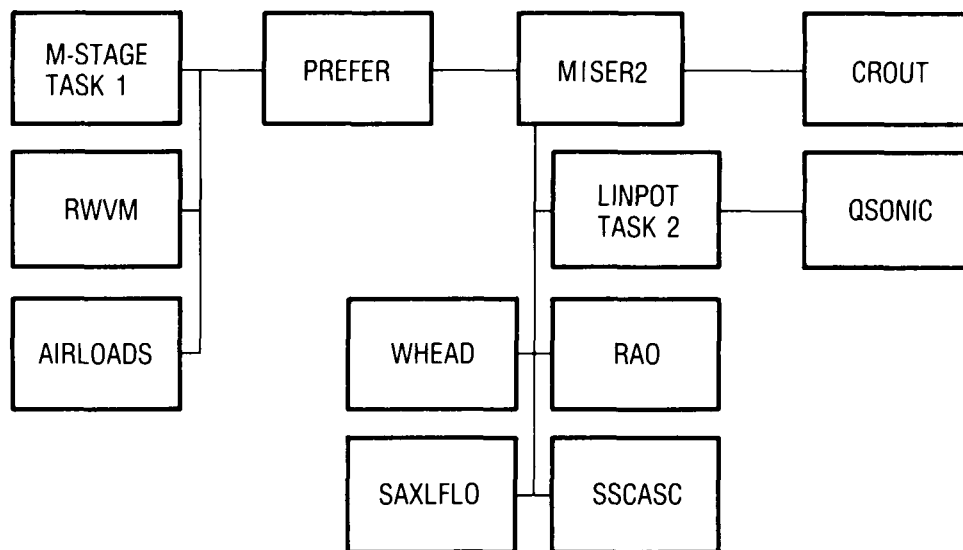


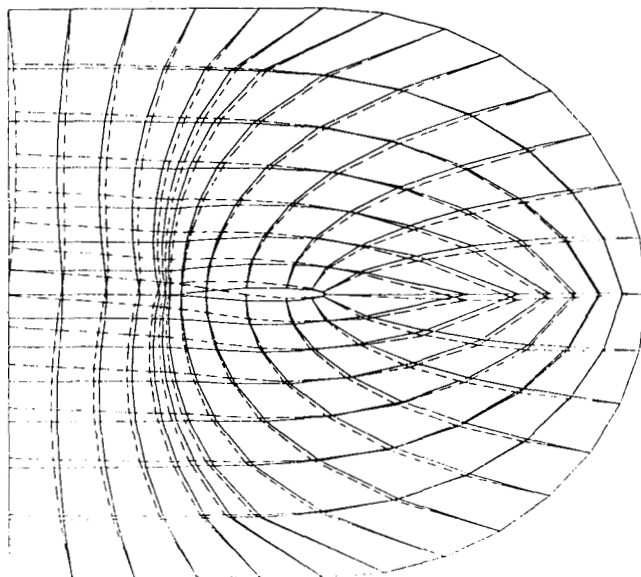
Figure 19

**ORIGINAL PAGE IS  
OF POOR QUALITY**

2D Unsteady, Viscous Cascade Aero Model

A compressible, unsteady, full Navier-Stokes, finite difference code has been developed for modeling transonic flow through two-dimensional, oscillating cascades. The procedure introduces a deforming grid (fig. 20) technique to capture the motion of the airfoils. The use of a deforming grid is convenient for treatment of the outer boundary conditions since the outer boundary can be fixed in space, while the inner boundary moves with the blade motion. The code is an extension of the isolated airfoil code developed in reference 20. More results validating the deforming grid technique are presented in reference 21.

2D UNSTEADY VISCOUS CASCADE AERO MODEL



2D UNSTEADY VISCOUS CASCADE AERO MODEL

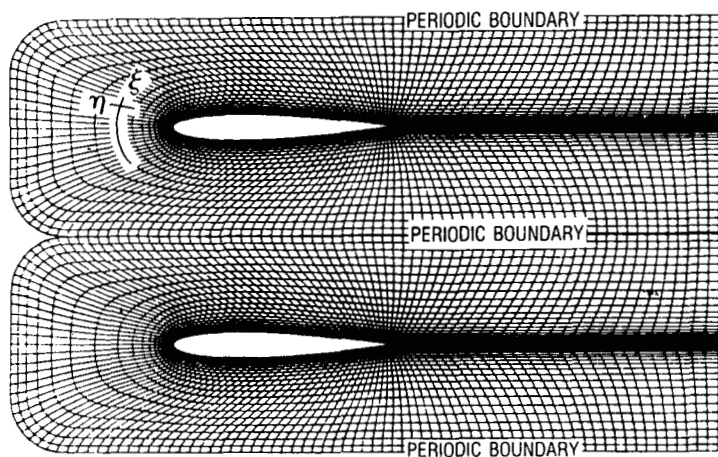


Figure 20

Pressure Coefficients for an NACA 0012 Cascade  
with Viscous Effects

The deforming grid technique has been used to predict the load histories for a NACA 0012 cascade with zero inter-blade phase angle and zero stagger. Two flow conditions were selected to investigate both subsonic and transonic flow. The cascade has a gap to chord ratio of one,  $M = 0.60$  and  $0.67$ ,  $Re = 3.21$  million,  $\alpha_m = 0.0$  degrees, pitching  $\pm 2.0$  degrees, and  $k = 0.20$  (reduced frequency based on semi-chord). A Fourier transform on the pressure coefficient distribution was done for the first harmonics. The results are shown in figure 21. Future work will investigate non-zero inter-blade phase angles and will compare predictions with experimental data from the NASA Lewis Transonic Oscillating Cascade Facility.

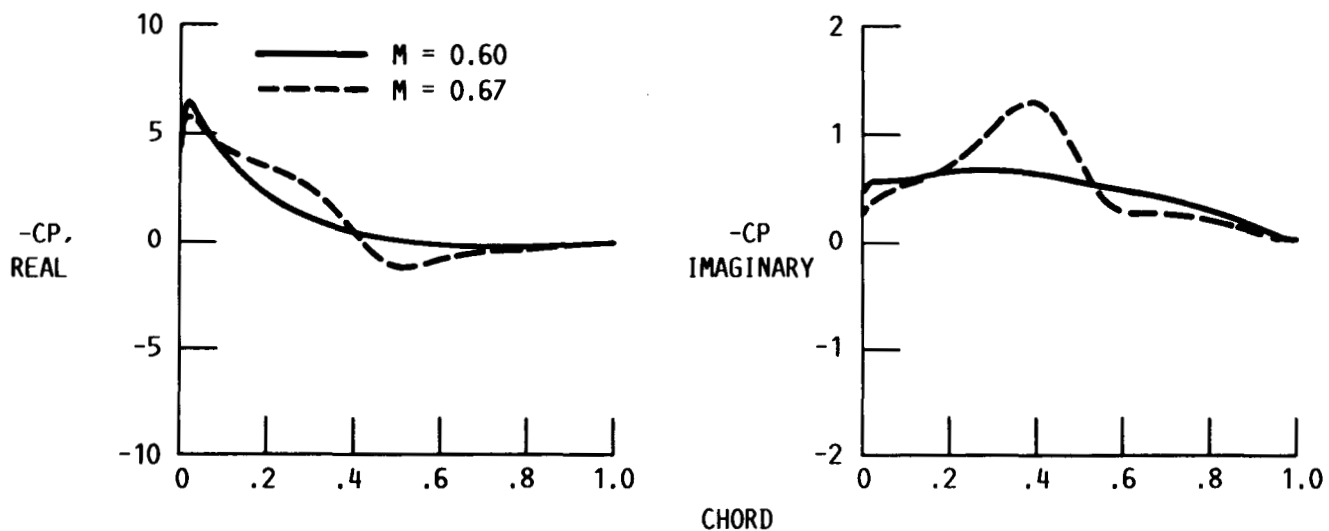


Figure 21

### 3-D Unsteady Euler Analysis

The three dimensional unsteady Euler analysis for an isolated wing developed in ref. 22 has been recently extended to propfans. This extended version of the code is being utilized to study the effect that propfan angle-of-attack has on the unsteady blade loading of a single rotation propfan design. The code is capable of modeling the complete propfan configuration. The program will be used to predict the unsteady loading on the propfan recently tested in a two-bladed configuration as part of the Large-Scale Advanced Propfan (LAP) program. Part of the objective of this test program was to obtain detailed steady and unsteady blade surface pressure measurements for benchmarking computer models. Presently this computer program assumes that the blades are rigid. It is planned to look at the formulation and coding necessary to allow the blades to respond to the unsteady loading thus allowing the program to be used in aeroelastic forced response predictions. Sample pressure contours on blades of a propfan are shown in figure 22.

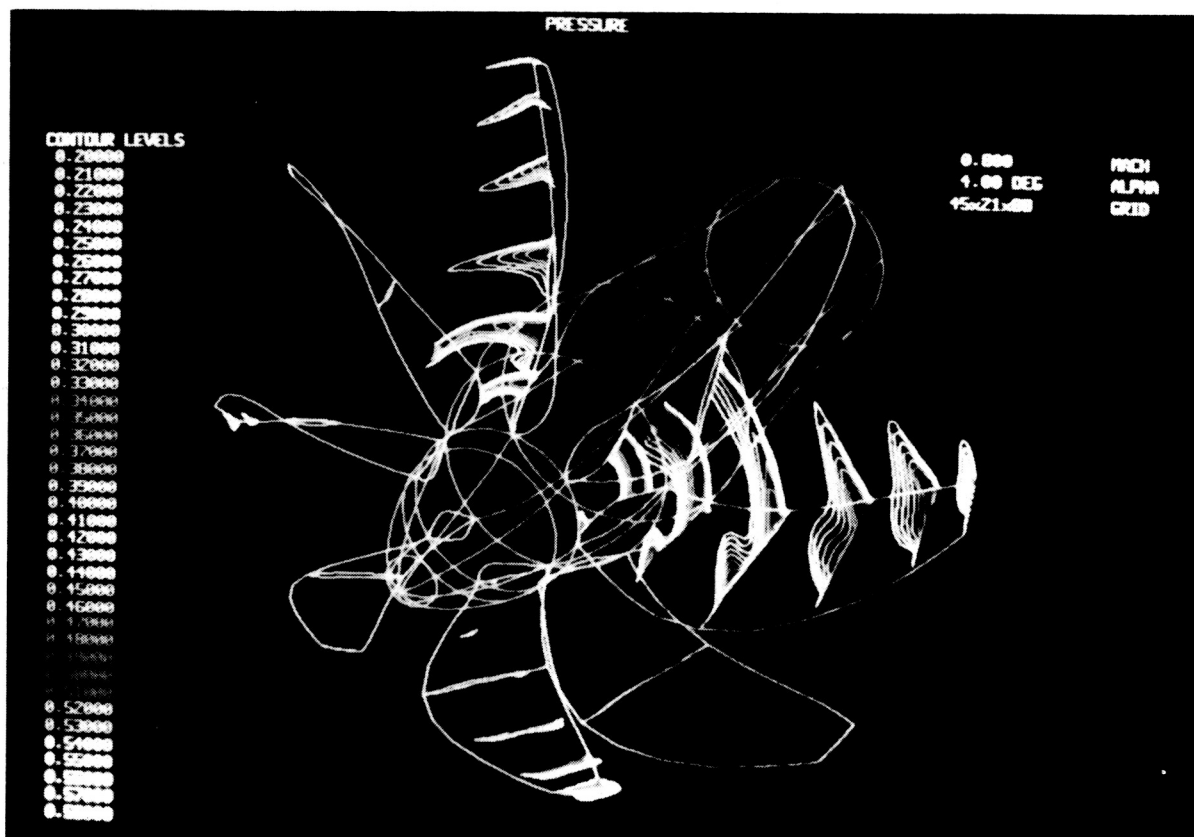


Figure 22

## 2-D Unsteady Perturbation Analysis for Cascades

In order to study the effect that blade sweep has on the flutter behavior of a cascade of airfoils operating in the transonic flow regime, the linearized unsteady analysis developed in ref. 17 is being utilized. This analysis predicts the unsteady loading resulting from small amplitude harmonic motion of the blades in a two-dimensional cascade operating in an inviscid subsonic or transonic flow. The unsteady potential is obtained from a perturbation analysis applied to the steady flow solution. Thus, the unsteady analysis is able to include the effects of finite mean loading on the unsteady response. At LeRC, the transonic potential code developed in reference 23 is utilized in calculating the steady flow field. Sample unsteady pressures calculated for a cascade of NACA 0012 airfoils (at Mach number 0.6, stagger angle  $45^\circ$  and mean incidence angle  $9^\circ$ ) by using the combined code are shown in figure 23. The combination of these steady and unsteady programs allows for the prediction of the flutter behavior of fan and propfan designs which include the effect of realistic reduced frequencies and blade geometries. The resulting computer program will be benchmarked against experimental cascade data and then applied to study the effect that blade sweep has on the flutter behavior of a cascade of airfoils.

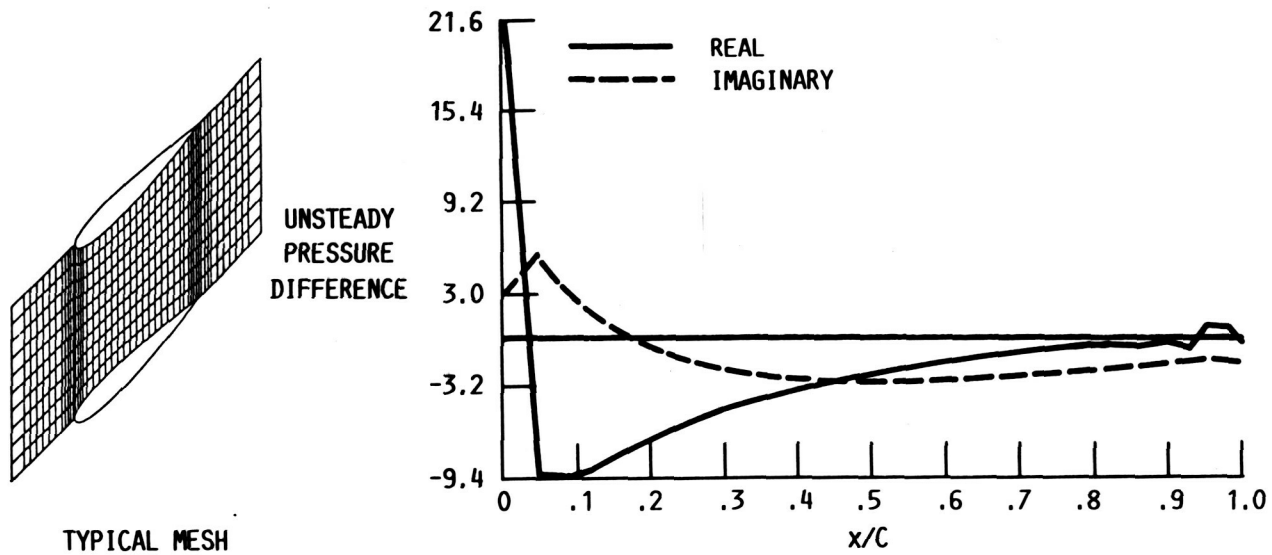


Figure 23

Unsteady Swept Cascade Experiments

The effect of blade sweep on the flutter behavior of a cascade of airfoils is being studied in the transonic oscillating cascade facility, figure 24. This study is being conducted to determine if classical sweep corrections applicable for fixed wing flows are valid for oscillating airfoils in a torsional motion while maintaining a selected interblade phase angle between adjacent blades. The unsteady loading is determined by a number of blade mounted high response pressure transducers. The initial phase of testing will involve the use of unswept airfoils in order to provide a baseline set of data for benchmarking the computer programs to be used in this study. The swept airfoils will then be installed and a series of tests will be run to determine the effect of incidence angle, Mach number, reduced frequency and interblade phase angle on the flutter behavior of the swept cascade.

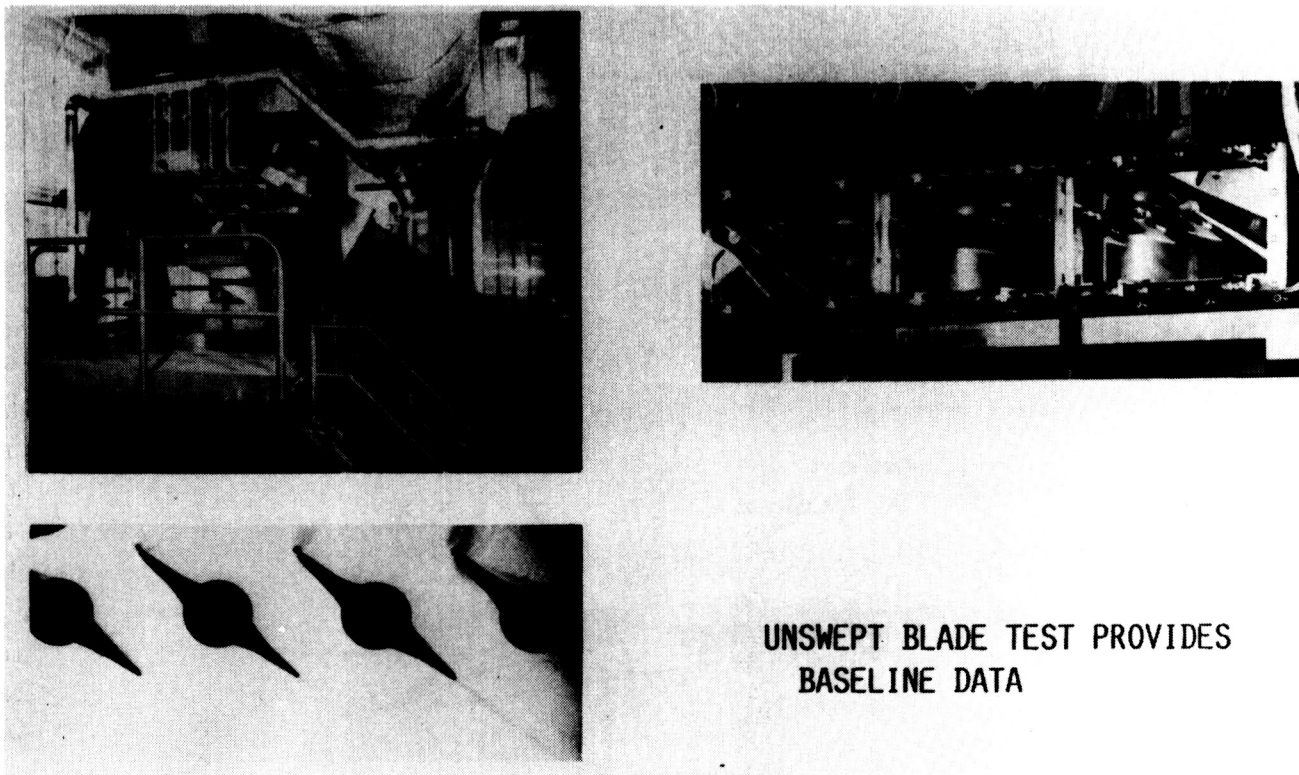


Figure 24

### Three-Dimensional Gust Model for a Propeller Blade

A propeller blade (figure 25) rotating in a nonuniform upstream flow encounters an unsteady flow field, even when the nonuniform upstream flow is steady. For straight bladed propellers, the unsteady flow of the propeller can be approximated by a two-dimensional wing in a three-dimensional gust as shown in figure 25. For small amplitude disturbances, the unsteady flow field may be obtained as a perturbation about the underlying steady flow. The governing equation is a linear, nonconstant coefficient, inhomogenous, convective wave equation, see refs. 24 and 25. A finite difference scheme is used to solve for the perturbation potential. Some sample results are shown in figure 26.

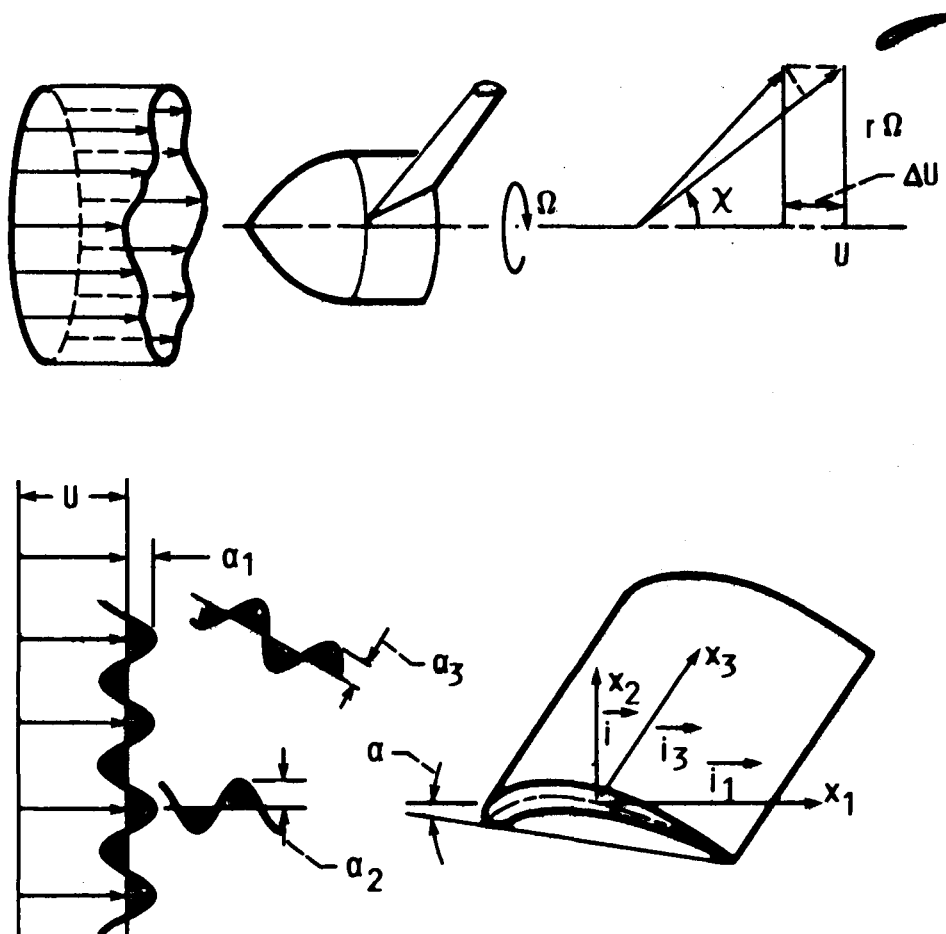


Figure 25

Variation of Unsteady Lift Coefficient  
of 12% Thick, Symmetric Joukowski  
Airfoil in a Transverse Gust

The governing wave equation for the model described in figure 25 is solved for perturbation potential by using a finite differencing scheme. For a symmetric airfoil in a transverse gust the real and imaginary parts of the lift at Mach number 0.6 and with reduced frequency as parameters are shown in figure 26. Also included in the figure is the corresponding curve for the flat plate. Comparing the flat plate and 12% thick airfoil results, it is observed that the thickness effects on the lift are more significant at low reduced frequencies. Similar comparisons (not shown) are also made at different Mach numbers, and it was found that the thickness effects on lift are more significant at higher Mach numbers.

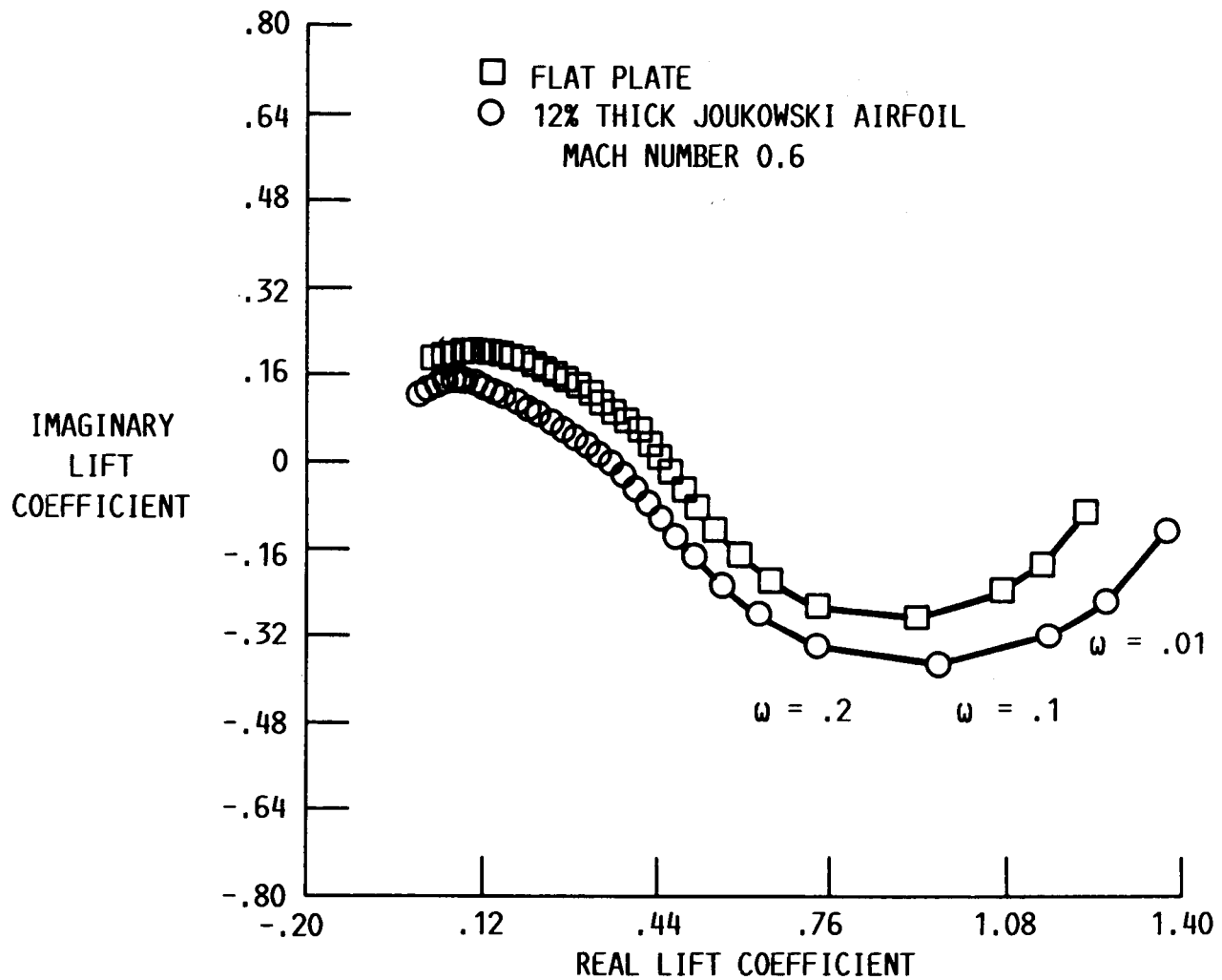
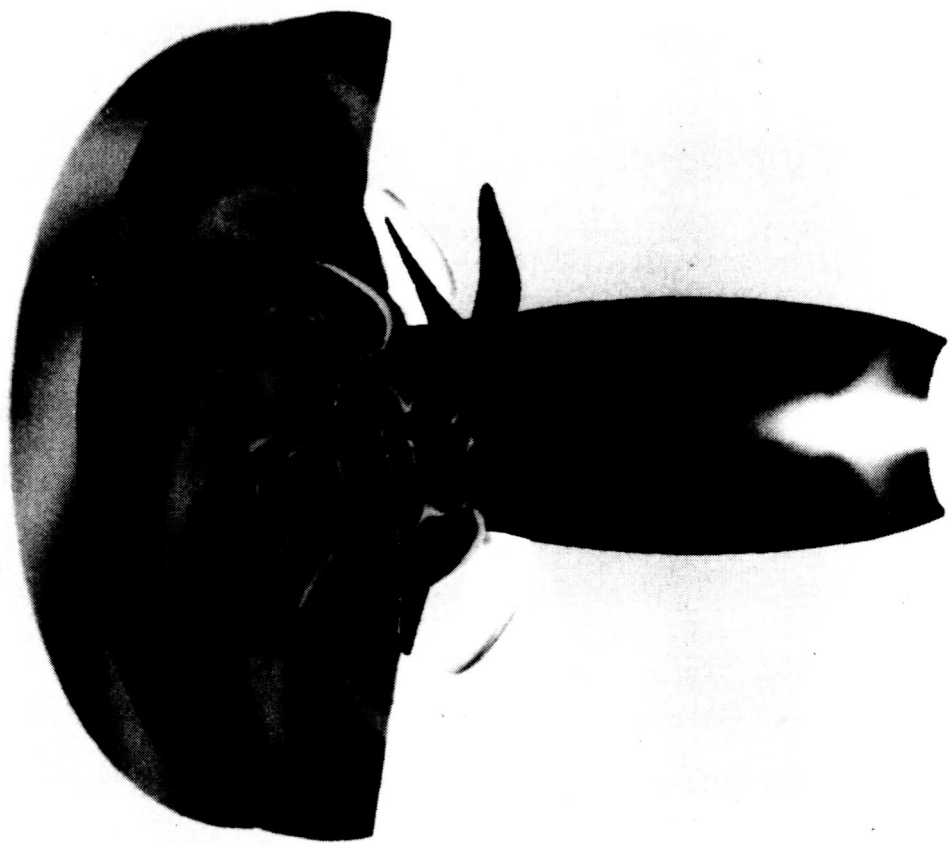


Figure 26

**ORIGINAL PAGE IS  
OF POOR QUALITY**

**Numerical Simulation of Flow Through  
Counter Rotating Propfans - Average  
Passage Flow Model**

A new analytical model, referred to as "average passage flow model," is being developed in reference 26 for simulating flows through counter rotating propfans. It describes the three-dimensional time-average flow field within a typical passage of a blade run in a multiblade run configuration. The model has been used to examine the flow field generated by a counter rotating propfan configuration (UDF). For example, the pressure field radiated by the aft fan is shown in figure 27. The pressure field is color-coded with a spectrum ranging from blue (low pressure) to green to yellow to red (high pressure). The boundary between green (lower pressure) and yellow-orange (higher pressure) regions is the footprint of the aft propfan trailing-edge shock. The base of the shock lies at approximately three-quarters of the span. From this point it appears to spiral outward beyond the tip of each blade.



**Figure 27**

Application of "Average Passage Flow Model"  
for CR Propfan Noise Prediction

The average passage flow model developed in ref. 26 was merged with an aeroacoustic prediction model for CR propfans developed by Dr. F. Farassat of NASA Langley Research Center. This merger permits the simultaneous evaluation of aerodynamic performance and radiated sound levels. Figure 28 shows a comparison of the predicted sound levels with corresponding measured data of the CR scaled model by Dr. J. H. Dittman of NASA Lewis Research Center. The correlation between theory and experiment is excellent.

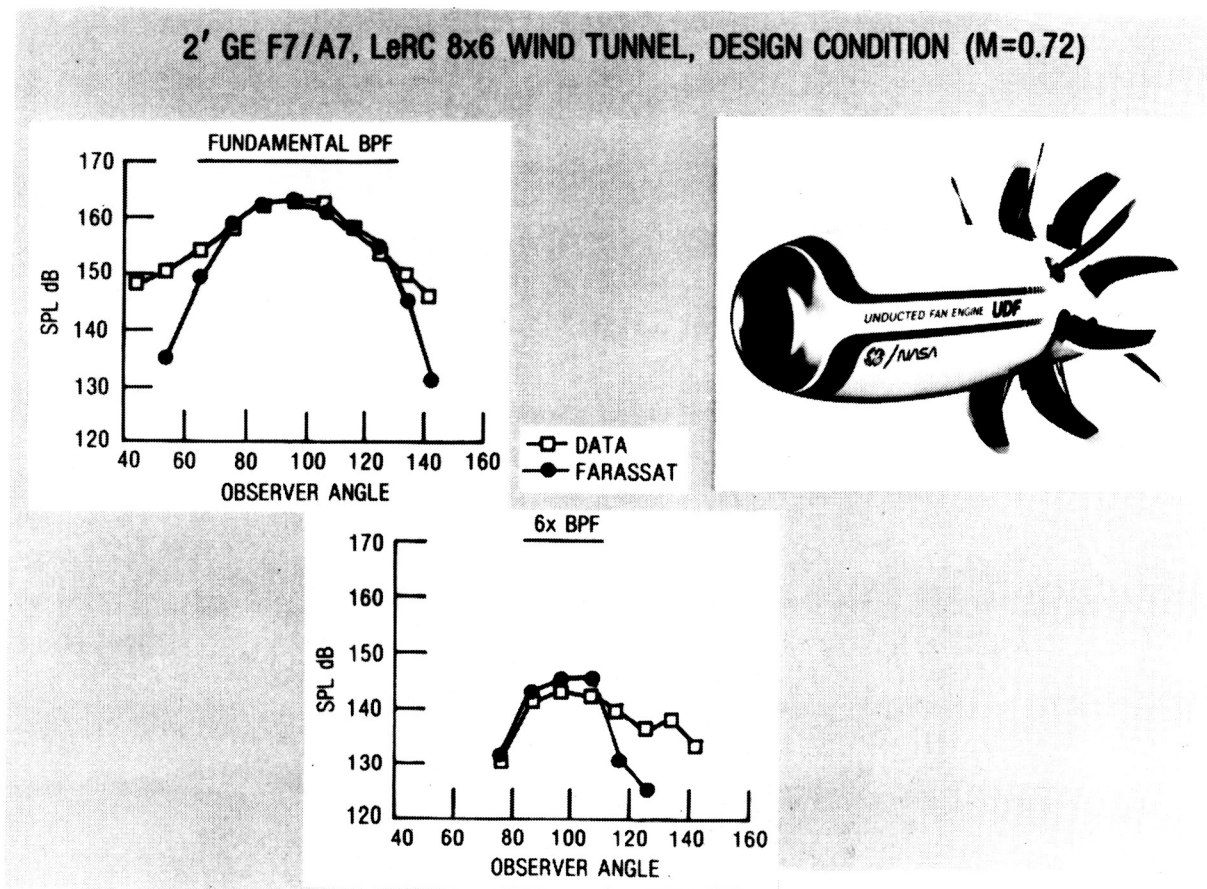


Figure 28

ORIGINAL PAGE IS  
OF POOR QUALITY

## LeRC Groups Involved in Unsteady Aerodynamics and Aeroelasticity

The groups in the unsteady aerodynamics and aeroelasticity effort at LeRC are shown in figure 29. Also listed in the figure are the names of NASA LeRC employees, Support Service Contractors and Grantees, who contributed to the research effort described in the paper.

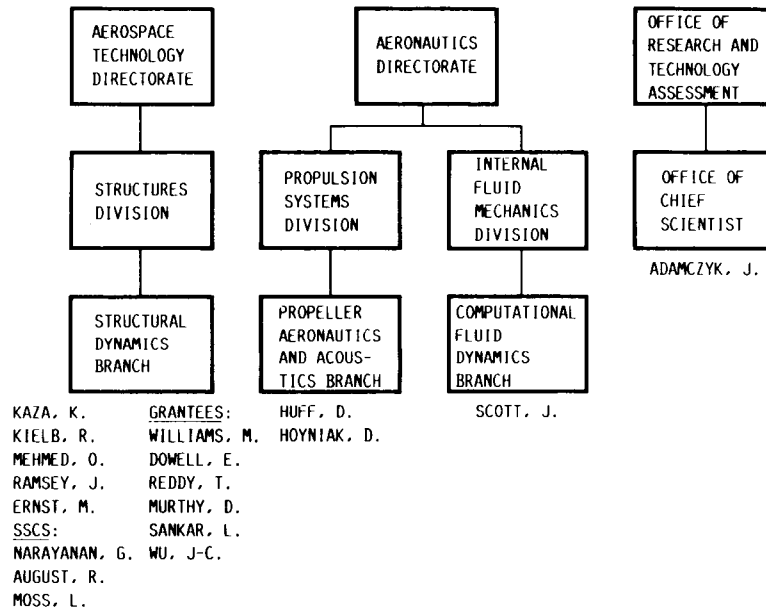
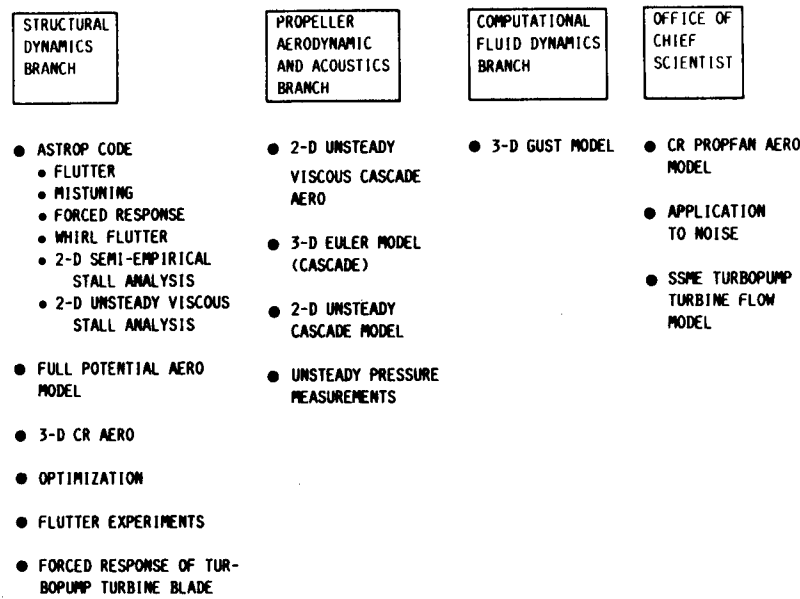


Figure 29

**ORIGINAL PAGE IS  
OF POOR QUALITY**

**LeRC Unsteady Aerodynamics and Aeroelasticity Effort**

The elements of the overall research effort in the subject area are shown in figure 30. These elements cover the development of unsteady aerodynamic models, aeroelastic models (for flutter, forced response and optimization), associated computer programs, and wind tunnel flutter experiments.



**Figure 30**

### References

1. Kaza, K.R.V., Mehmed, O., Narayanan, G.V., and Murthy, D.V.: Analytical Flutter Investigation of a Composite Propfan Model. NASA TM 88944 1987, AIAA Paper No. 87-0738.
2. Williams, M.H., and Hwang, C.: Three Dimensional Unsteady Aerodynamics and Aeroelastic Response of Advanced Turboprops. AIAA 27th SDM Conference, part II, 1986, pp. 116-124.
3. The Nastran Theoretical Manual, NASA SP-221(06) 1981.
4. Chamis, C.C.: "Integrated Analysis of Engine Structures. NASA TM-82713, 1981.
5. Mehmed, O., and Kaza, K.R.V.: Experimental Classical Flutter Results of a Composite Advanced Turboprop Model. NASA TM-88972, 1986.
6. Rao, B.M., and Jones, W.P.: Unsteady Airloads for a Cascade of Staggered Blades in Subsonic Flow. Unsteady Phenomena in Turbomachinery, AGARD CP-177, AGARD, France, 1976, pp. 32-2 to 32-10.
7. Kaza, K.R.V., Mehmed, O., Williams, M., and Moss, L.: Analytical and Experimental Investigation of Mistuning in Propfan Flutter. NASA TM 88959 1987, AIAA Paper No. 87-0739.
8. Mehmed, O., Kaza, K.R.V., Lubomski, J.F., and Kielb, R.E.: Bending Torsion Flutter of Highly Swept Advanced Turboprop. NASA TM 82975, 1982.
9. Elchuri, V.: Modal Forced Vibration Analysis of Aerodynamically Excited Turbosystems. NASA CR 174966, July 1985.
10. Reddy, T.S.R., and Kaza, K.R.V.: A Comparative Study of Some Dynamic Stall Models. NASA TM 88917, 1987.
11. Gormont, R.E.: A Mathematical Model of Unsteady Aerodynamics and Radial Flow for Application to Helicopter Rotors. USAAMRDL TR-72-67, May 1973.
12. Gangwani, S.T.: Prediction of Dynamic Stall and Unsteady Airloads for Rotor Blades. J. Of American Helicopter Society, Vol. 27, No. 4, October 1982, pp. 57-64.
13. Wu, J.-C., and Kaza, K.R.V., and Sankar, L.N.: A Technique for the Prediction of Airfoil Flutter Characteristics in Separated Flow. AIAA Paper No. 87-0910-CP, 1987.
14. Farr, J.L., Traci, R.M., and Albano, E.D.: Computer Programs for Calculating Small Disturbance Transonic Flows About Oscillating Airfoils. AFFDL-TR-74-135, Nov. 1974.
15. Guruswami, D.M., and Yang, T.Y.: Transonic Time-Response Analysis of Thin Airfoils by Transonic Code LTRAN2. Computers and Fluids, Vol. 9, No. 4, pp. 409-425, 1981.

16. Smith, S.N.: Discrete Frequency Sound Generation in Axial Flow Turbomachines. A.R.C. R&M No. 3709, 1973.
17. Verdon, J.M., and Caspar, J.R.: "A Linearized Unsteady Aerodynamic Analysis for Transonic Cascades. NASA CR 168638.
18. Chen, S.H., and Williams, M.H.: Panel Method for Counter Rotating Propfans. AIAA Paper No. 87-1890, 1987.
19. Lesieurte, D.J., and Sullivan, J.P.: Unsteady Forces on Counter-Rotating Propeller Blades. AIAA Paper No. 86-1804, 1986.
20. Sankar, L.N., and Tang, W.: Numerical Solution of Unsteady Viscous Flow Past Rotor Sections. AIAA Paper No. 85-0129.
21. Huff, D.: Numerical Simulations of Unsteady, Viscous, Transonic Flow over Isolated and Cascaded Airfoils Using a Deforming Grid. AIAA Paper No. 87-1316, 1987.
22. Whitefield, D.L., and Janus, J.M.: Three Dimensional Unsteady Euler Equations Solution Using Flux Vector Splitting. AIAA 84-1552, June 1981.
23. Farrel, C., and Adamczyk, J.: Full Potential Solution of Transonic Quasi-Three-Dimensional Flow Through a Cascade Using Artificial Compressibility. Journal of Engineering for Power, Jan. 1982, Vol. 104, pp. 143-153.
24. Goldstein, M.E.: Unsteady Vortical and Entropic Distorsions of Potential Flows Round Arbitrary Obstacles. J. Fluid Mech., Vol. 89, Part 3, 1978, pp. 433-468.
25. Atassi, H.M., and Grzedzinski, J.: Unsteady disturbances of Streaming Motions Around Bodies. To appear in J. of Fluid Mechanics, 1987.
26. Adamczyk, J.F.: Model Equations for Simulating Flows in Multistage Turbomachinery. ASME Paper No. 85-GT-226, March 1985.